GEOPHYSICAL RESEARCH LETTERS, VOL. 35, L09706, doi:10.1029/2008GL033567, 2008

Radiative forcing over the conterminous United States due to contemporary land cover land use albedo change

Christopher A. Barnes[1] and David P. Roy[1]

Received 6 February 2008; revised 28 March 2008; accepted 4 April 2008; published 9 May 2008.

[1] Recently available satellite land cover land use (LCLU) and albedo data are used to study the impact of LCLU change from 1973 to 2000 on surface albedo and radiative forcing for 36 ecoregions covering 43% of the conterminous United States (CONUS). Moderate Resolution Imaging Spectroradiometer (MODIS) snow-free broadband albedo values are derived from Landsat LCLU classification maps located using a stratified random sampling methodology to estimate ecoregion estimates of LCLU induced albedo change and surface radiative forcing. The results illustrate that radiative forcing due to LCLU change may be disguised when spatially and temporally explicit data sets are not used. The radiative forcing due to contemporary LCLU albedo change varies geographically in sign and magnitude, with the most positive forcings (up to 0.284 Wm^{-2}) due to conversion of agriculture to other LCLU types, and the most negative forcings (as low as -0.247 Wm^{-2}) due to forest loss. For the 36 ecoregions considered a small net positive forcing (i.e., warming) of 0.012 Wm^{-2} is estimated. **Citation:** Barnes, C. A., and D. P. Roy (2008), Radiative forcing over the conterminous United States due to contemporary land cover land use albedo change, *Geophys. Res. Lett.*, *35*, L09706, doi:10.1029/2008GL033567.

1. Introduction

[2] Land cover land use (LCLU) affects Earth surface properties including albedo that impose a radiative forcing on the climate. It is thought that LCLU change during the twentieth century has induced a net cooling effect on mid latitude climate [*Oleson et al.*, 2004; *Gibbard et al.*, 2005] and globally has resulted in a radiative forcing of approximately -0.25 Wm^{-2} [*Intergovernmental Panel on Climate Change* (*IPCC*), 2007]. Albedo changes due to LCLU depend on both the type and spatial extent of LCLU change, and the spatial averaging of opposite signs of LCLU forcing may under represent LCLU contributions over larger areas [*Pielke et al.*, 2002; *Kleidon*, 2006]. Previous studies have considered hypothetical LCLU change scenarios using representative albedo values. For example, *Betts* [2000] simulated a net climate warming influence with boreal afforestation in the presence of snow, and *Bala et al.* [2007] simulated a net cooling influence with large scale global deforestation. Satellite driven studies have been undertaken using spatially and/or temporally explicit albedo retrievals but have not considered contemporary LCLU change [*Jin and Roy*, 2005; *Myhre et al.*, 2005; *Randerson et al.*, 2006]. In this paper we quantify the surface radiative forcing of contemporary LCLU albedo change (1973 to 2000) for 43% of the conterminous United States (CONUS) using recently available satellite derived LCLU change and albedo data.

2. Data

[3] Classification techniques are being used to generate 60 m LCLU maps from Landsat scenes located within 84 contiguous ecoregions across the CONUS [*Loveland et al.*, 2002; P. Jellison and W. Acevedo, United States Geological Survey Land Cover Trends Project, unpublished data, 2008]. The Landsat data are classified by visual interpretation, inspection of aerial photography and ground survey, into 10 classes (Table 1). The classes are defined to capture LCLU discernable in Landsat data. Each ecoregion includes 9 to 48 Landsat 10 km $\times$ 10 km or 20 km $\times$ 20 km classified spatial subsets located using a stratified random sampling methodology that are used to estimate areal LCLU class proportions [*Stehman et al.*, 2005]. At the time of writing only 36 of the 84 ecoregions have been processed by the United States Geological Survey and these are used in this study. The ecoregion areal LCLU class proportions and classified Landsat subsets defined for 1973 and for 2000 are considered. The 36 ecoregions are illustrated in Figure 1 and cover 43% of the CONUS; the classified Landsat subsets cover 3.7% of this area.

[4] Albedo data are provided by the most recent Moderate Resolution Imaging Spectroradiometer (MODIS) Collection 5 BRDF/Albedo 16-day 500 m product [*Schaaf et al.*, 2002] that is available every 8 days [*Roy et al.*, 2006]. Three years of 500 m (0.3–5.0 μm) snow-free broadband white sky albedo data (February 18th 2000 to February 18th 2003) are used to capture inter-annual albedo variability.

[5] The European Center for Medium-Range Weather Forecasts (ECMWF) 40 year Reanalysis data set (ERA40) provides global monthly mean incoming surface solar radiation (SSRD) at 2.5° by 2.5° grid cells from September 1957 to August 2002 [*Allan et al.*, 2004]. Data from January 1973 to December 2000 are used to derive mean monthly SSRD for each ecoregion.

3. Method

[6] Monthly albedos for each ecoregion were estimated independently for 1973 and 2000 as:

$$\alpha_{ecoregion,\,month,\,year} = \sum_{class\ i=1}^{10} \left(P_{i,\,ecoregion,\,year}\ \bar{\alpha}_{i,\,ecoregion,\,month} \right) \quad (1)$$

[1]Geographical Information Science Center of Excellence, South Dakota State University, Brookings, South Dakota, USA.

0094-8276/08/2008GL033567$05.00

Table 1. Ten LCLU Classes, the LCLU Class Areal Proportions for 1973 and 2000, and the Net Change From 1973 to 2000, for the 36 CONUS Ecoregions Considered in This Study[a]

LCLU Class	1973 LCLU, km^2	2000 LCLU, km^2	LCLU Change 1973–2000, %
Water	86298	88618	0.07
Developed (e.g., residential and industrial land uses)	164579[b]	211232[b]	1.35[b]
Mechanically disturbed	20512	43737	0.67
Mining	9854	10742	0.03
Barren	32463	32740	0.01
Forest	1142148	1094247	−1.39
Grass/shrubland	1156826	1182751	0.75
Agriculture	695532[b]	644747[b]	−1.47[b]
Wetland	139567	133384	−0.18
Naturally disturbed	2075	7638	0.16

[a]See Figure 1.
[b]The greatest net LCLU changes.

where, for each LCLU class i, p_i is the LCLU class area proportion, and $\bar{\alpha}_i$ is the mean monthly snow-free broadband white sky MODIS albedo derived from the three years of MODIS data. The albedo values were derived at locations defined by the Landsat 2000 classified subsets. To ensure that MODIS 500 m pixels containing only a single LCLU class were considered, the boundaries of the LCLU classes in each subset were morphologically eroded by 240 m [*Serra*, 1982]. Albedo values were then extracted at the remaining LCLU class centroids for 3 years of snow-free non-missing MODIS data every 8 days after the Landsat 2000 acquisition date to February 18th 2003. A total of 197,205 MODIS albedo values were extracted and used in this study. In some ecoregions, for certain LCLU classes and months, there were insufficient MODIS data to compute $\bar{\alpha}_i$; this typically occurred in ecoregions with small areal LCLU class proportions (<0.005) in cloudy and snow contaminated months. In these cases, and when $p_i > 0$, $\bar{\alpha}_i$ was set as the median of the mean monthly class albedos computed for the ecoregions with available MODIS data.

[7] The monthly surface radiative forcing ($\Delta F_{surface,\,month}$) in each ecoregion due to LCLU induced albedo change, defined as the instantaneous change in energy flux at the surface [*Hansen et al.*, 1997], was estimated as:

$$\Delta F_{ecoregion,month} = -\bar{I}^{\downarrow}_{ecoregion,month} \cdot \left(\alpha_{ecoregion,month,2000} - \alpha_{ecoregion,month,1973}\right) \quad (2)$$

where $\bar{I}^{\downarrow}$ is the mean monthly incoming surface solar radiation [Wm^{-2}] derived from the ERA40 dataset, and α_{2000} and α_{1973} are the monthly ecoregion albedos for 2000 and 1973 respectively (equation (1)). The mean annual

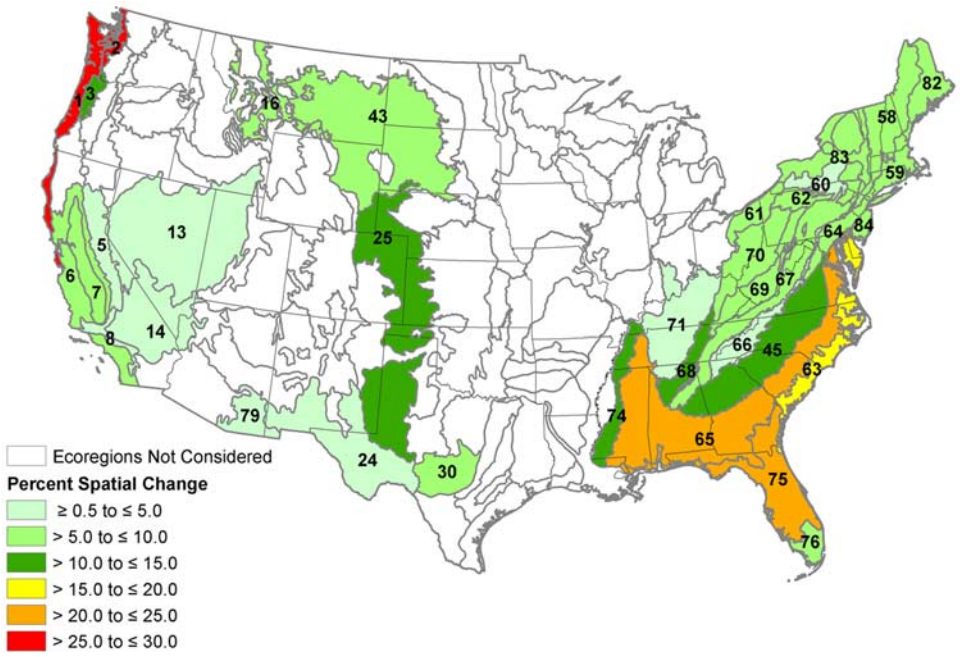

Figure 1. The 36 ecoregions, available to date, used in this study (numbered and colored) and their proportions of land cover and land use (LCLU) change, from 1973 to 2000 (P. Jellison and W. Acevedo, unpublished data, 2008).

Table 2. Mean and Standard Deviation of Snow−Free Broadband White Sky Albedos for Each Land Cover Land Use LCLU Class Computed Over the 36 CONUS Ecoregions Considered in This Study From 3 Years of MODIS Data[a]

LCLU Class	Mean of CONUS Albedos	Standard Deviation of CONUS Albedos	*n*	Minimum Within Ecoregion Albedo Standard Deviation	Median Within Ecoregion Albedo Standard Deviation	Maximum Within Ecoregion Albedo Standard Deviation
Barren	0.240	0.095	1727	0.059	0.068	0.077
Agriculture	0.171	0.026	47484	0.015	0.019	0.033
Grassland/shrubland	0.168	0.039	34597	0.014	0.023	0.047
Mining	0.153	0.038	4818	0.013	0.023	0.039
Developed	0.150	0.030	24297	0.014	0.018	0.034
Mechanically disturbed	0.138	0.027	8501	0.016	0.019	0.025
Forest	0.128	0.026	50821	0.014	0.022	0.031
Wetland	0.127	0.028	12731	0.016	0.024	0.044
Naturally disturbed	0.120	0.026	732	0.017	0.017	0.018
Water	0.058	0.043	11497	0.016	0.028	0.038

[a]See Figure 1; *n* is the number of albedo values considered; the LCLU classes are ranked in descending mean albedo order. The minimum, median, and maximum albedo standard deviations are also shown to indicate the variability of within ecoregion albedo.

forcing for each ecoregion was derived as the mean of the 12 monthly forcings.

4. Results

[8] For the 36 CONUS ecoregions considered, the dominant contemporary (1973–2000) LCLU changes were a net areal increase in developed land (1.35%) and a net decrease in agricultural land (−1.47%) (Table 1). The most extensive LCLU changes occurred in the Pacific Northwest (>25%) and in the Southeast (>20%), and the least (<5%) in the Central Basin region (Figure 1). This pattern of LCLU change is driven primarily by socio-economic factors causing exurban sprawl [*Theobold*, 2005] and the conversion and abandonment of agricultural land mainly for development [*Brown et al.*, 2005].

[9] Table 2 summarizes the CONUS MODIS 3 year mean snow-free broadband white sky albedos for each LCLU class. The mean CONUS albedo class values are broadly comparable to other worker's results [*Myhre et al.*, 2005], with the barren and agriculture classes having the highest mean albedo (0.240 and 0.171 respectively) and the water class the lowest mean albedo (0.058). The CONUS standard deviation albedo values and the minimum, median, and maximum within-ecoregion standard deviations for each LCLU class are also tabulated, and are indicative of geographic albedo variation. The CONUS standard deviations for the different classes are always greater than the median within-ecoregion albedo standard deviations, but are not significantly smaller than the maximum within-ecoregion albedo standard deviations. This in part reflects noise in the MODIS data, but is not unexpected as the ecoregion LCLU stratification was not designed with respect to albedo directly, and because albedo varies as a function of numerous factors not captured by the LCLU classes. For example, the forest class is present in all the ecoregions considered,

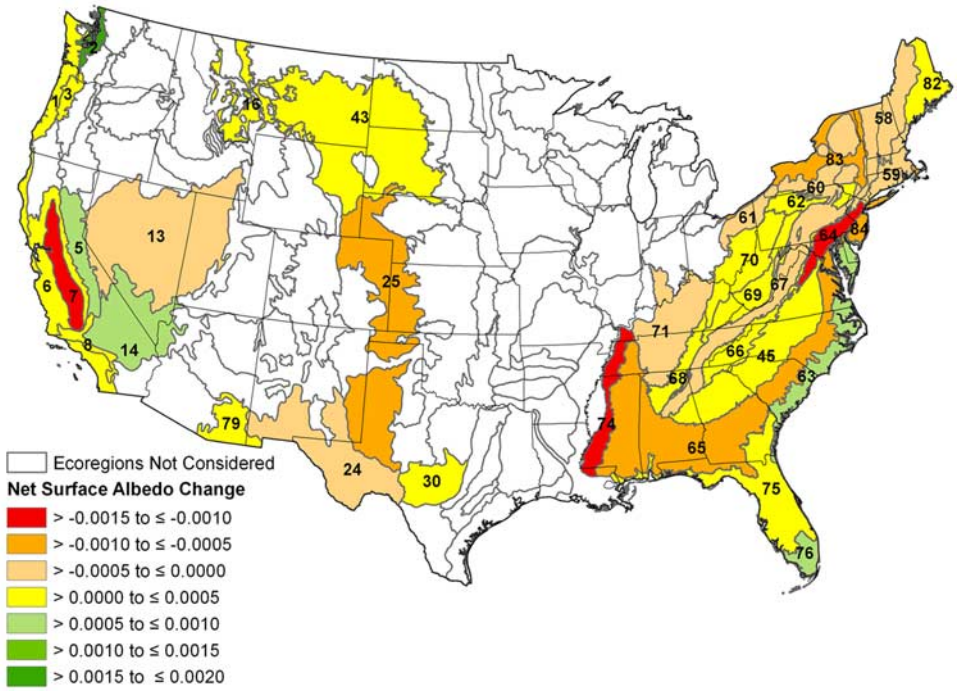

Figure 2. The estimated net albedo change due to contemporary land cover and land use (LCLU) change from 1973 to 2000 ($\alpha_{2000} - \alpha_{1973}$) for the 36 ecoregions used in this study.

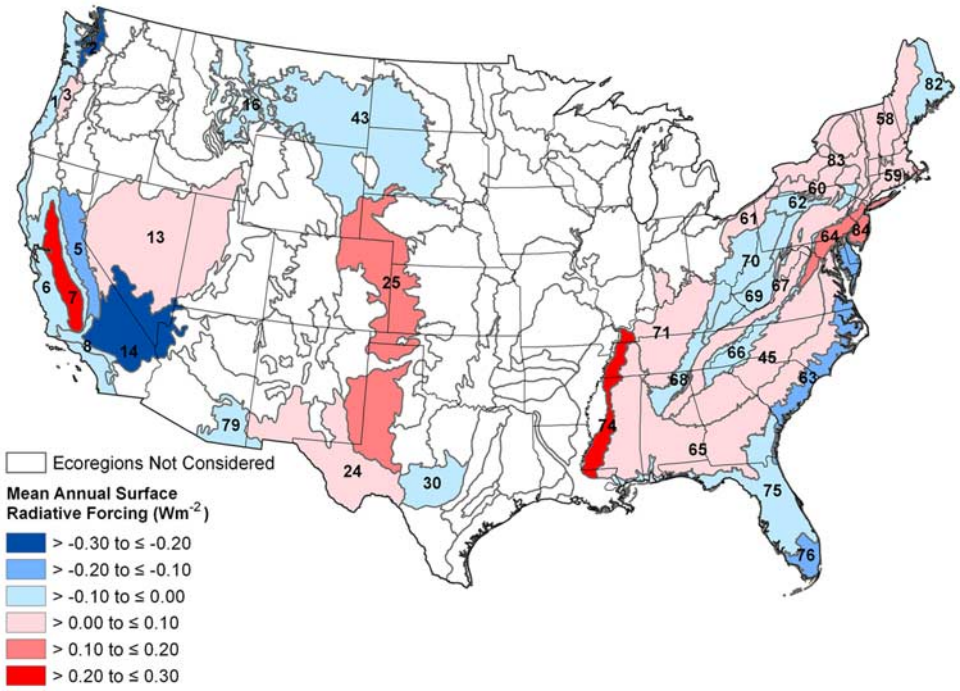

Figure 3. The mean annual surface radiative forcing due to contemporary land cover and land use (LCLU) albedo change from 1973 to 2000 (equation (2)) for the 36 ecoregions used in this study.

except for the Western High Plains (ecoregion 25), and encompasses a wide variety of tree species, stand densities, ages, and soil backgrounds. By using ecoregion specific mean monthly albedo values in equation (1) we reduce this geographic variability.

[10] The net changes in ecoregion albedo due to LCLU change are illustrated in Figure 2. The albedos of the LCLU classes and the extent of LCLU change determine these results; consequently ecoregions with the highest areal proportions of LCLU change (Figure 1) do not consistently coincide with the ecoregions of highest albedo change (Figure 2) and the correlation between these data is low (0.189). Timber harvesting in the Puget Lowland (ecoregion 2) produced the largest albedo increase (0.0016), whereas the conversion of agricultural land to forest in the Mississippi Valley Loess Plains (ecoregion 74) produced the largest decrease in albedo (−0.0015). To put these albedo changes into context, the mean annual SSRD for the 36 ecoregions considered is 190 Wm^{-2}; thus, a change in albedo of 0.0015 represents a surface forcing of 0.285 Wm^{-2}, which is not insignificant. Rather than apply continental annual averages however, equation (2), is used to compute surface forcings in an ecoregion specific manner using monthly data.

[11] Figure 3 illustrates the mean annual surface radiative forcing computed using ecoregion specific and monthly data (equation (2)). The surface radiative forcing ranged from −0.247 Wm^{-2} in the Puget Lowland (ecoregion 2) to 0.284 Wm^{-2} in the Mississippi Valley Loess Plains (ecoregion 74). The geographic distribution of forcing is highly correlated (−0.984) with the LCLU albedo change and only weakly (−0.119) correlated with the mean annual SSRD. Table 3 summarizes the five ecoregions with the highest observed positive and negative surface radiative forcings. The LCLU changes that resulted in the net largest magnitude of albedo change are also summarized (Table 3, column 5) and may not necessarily be the most extensive LCLU changes; for example, LCLU change between classes with very different albedos may have a greater net albedo impact than more extensive changes between classes with similar albedos. All five ecoregions with the highest positive radiative forcings experienced a LCLU conversion from agriculture (to forest, developed, or grass/shrub), whereas forest loss was a common conversion in the five ecoregions with the most negative forcings.

[12] Figure 4 shows a histogram of the mean annual surface radiative forcing values illustrated in Figure 3. The histogram shape illustrates an almost balanced distribution of positive and negative forcing for the 36 ecoregions (mean 0.001 Wm^{-2}, median −0.006 Wm^{-2}). A CONUS scale forcing estimate, derived by summing the product of the ecoregion areas (m^2) and forcing estimates (Wm^{-2}), divided by the total area (m^2) of the 36 ecoregions, provides a small positive (i.e. warming) net surface radiative forcing of 0.012 Wm^{-2}.

5. Summary

[13] This letter has demonstrated the value of regional spatially and temporally explicit data to quantify, and begin to understand, the drivers of LCLU related radiative forcing which remains poorly understood [*Pielke et al.*, 2002; *National Research Council*, 2005; *IPCC*, 2007]. Previous United States historical [*Bounoua et al.*, 2002; *Matthews et al.*, 2003] and contemporary [*Hale et al.*, 2006] LCLU climate studies have indicated directional uncertainty in radiative forcing estimates. Our results also indicate this, with a large geographic variation in forcing due to

Table 3. Five Ecoregions That Observed the Highest Mean Annual Positive and Negative Radiative Forcing, Their Corresponding Mean Monthly Incoming Surface Solar Radiation (SSRD), Net Mean Annual Surface Albedo Change ($\alpha_{2000} - \alpha_{1973}$), and the Land Cover Land Use LCLU Change That Resulted in the Net Largest Magnitude of Albedo Change From 1973 to 2000[a]

Ecoregion	Mean Annual Surface Radiative Forcing, Wm^{-2}	Mean Annual Monthly SSRD, Wm^{-2}	Net Mean Annual Surface Albedo Change ($\alpha_{2000} - \alpha_{1973}$)	LCLU Change Conversion From/To
		Positive Radiative Forcing		
Mississippi Valley Loess Plain (74)	0.284	194	−0.00149	Agriculture to Forest
Central California Valley (7)	0.236	226	−0.00102	Agriculture to Grass/Shrub
Northern Piedmont (64)	0.164	177	−0.00100	Agriculture to Developed
Atlantic Coastal Pine Barrens (84)	0.156	180	−0.00088	Agriculture to Developed
Western High Plains (25)	0.140	212	−0.00064	Agriculture to Grass/Shrub
		Negative Radiative Forcing		
Puget Lowland (2)	−0.247	151	0.00156	Forest to M. Disturbed
Mojave Basin and Range (14)	−0.210	244	0.00089	Grass/Shrub to Developed
Sierra Nevada (5)	−0.153	221	0.00082	Forest to M. Disturbed
Southern Florida Coastal Plain (76)	−0.132	202	0.00067	Wetland to Agriculture
Middle Atlantic Coastal Plain (63)	−0.127	191	0.00068	Forest to M. Disturbed

[a]Ecoregion numbering is included in Figure 1.

LCLU albedo change, varying from -0.247 Wm^{-2} to 0.284 Wm^{-2}, for 36 ecoregions covering 43% of the CONUS. At the ecoregion level this magnitude of forcing is not insignificant, being similar in magnitude to global forcing estimates due to LCLU change during the twentieth century [*IPCC*, 2007].

[14] Loss of agricultural and forested lands were observed to be the LCLU changes that caused the greatest absolute albedo induced forcing. Across the CONUS however there is no single profile of LCLU change, rather, there are varying pulses affected by clusters of change agents [*Loveland et al.*, 2002]. This argues strongly for the ecoregion based analysis we have described, as continental averages may mask regional differences; indeed, because of the variability in magnitude and sign of forcing, we estimate only a small, 0.012 Wm^{-2}, net CONUS forcing due to contemporary LCLU albedo change. This work did not consider snow, which may have a significant land cover dependent albedo effect [*Jin et al.*, 2002] and so may impact the forcing associated with actual albedo change [*Betts*, 2000]; however, only about one eighth of the CONUS ecoregions considered in this study have significant annual snow cover. Further research will be undertaken to address these impacts for a larger number of ecoregions as more LCLU change data become available.

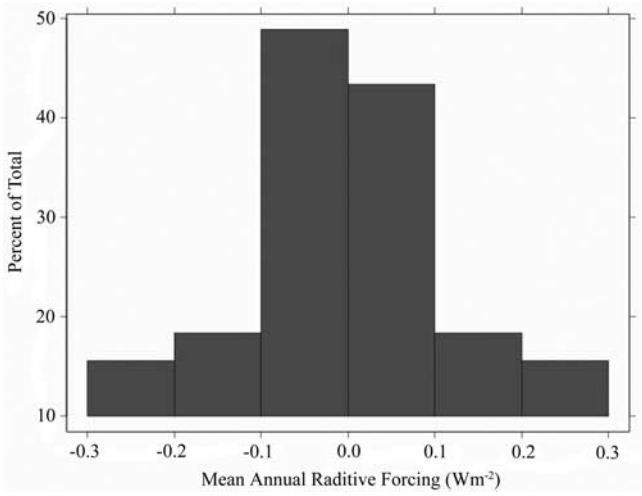

Figure 4. Histogram of the mean annual surface radiative forcing due to contemporary land cover and land use (LCLU) albedo change from 1973 to 2000 for the 36 ecoregions used in this study (Figure 3 data).

[15] **Acknowledgments.** The LCLU and the ERA-40 data used in this study were provided by the United States Geological Survey Earth Resources Observation and Science Center and by European Centre for Medium-Range Weather Forecasts respectively. This work was funded by NASA Grant NNX06AF87H. We acknowledge the helpful comments made by the reviewers to improve this letter.

References

Allan, R. P., M. A. Ringer, J. A. Pamment, and A. Slingo (2004), Simulation of the Earth's radiation budget by the European Centre for Medium-Range Weather Forecasts 40-year reanalysis (ERA40), *J. Geophys. Res.*, *109*, D18107, doi:10.1029/2004JD004816.

Bala, G., K. Caldeira, M. Wickett, T. J. Phillips, D. B. Lobell, C. Delire, and A. Mirin (2007), Combined climate and carbon-cycle effects of large-scale deforestation, *Proc. Natl. Acad. Sci. U.S.A.*, *104*, 6550–6555.

Betts, R. (2000), Offset of the potential carbon sink from boreal forestation by decreases in surface albedo, *Nature*, *408*, 187–190.

Bounoua, L., R. DeFries, G. J. Collatz, P. Sellers, and H. Khan (2002), Effects of land cover conversion on surface climate, *Clim. Change*, *52*, 29–64.

Brown, D. G., K. M. Johnson, T. R. Loveland, and D. M. Theobald (2005), Rural land use trends in the conterminous United States, 1950–2000, *Ecol. Appl.*, *15*, 1851–1863.

Gibbard, S., K. Caldeira, G. Bala, T. J. Philips, and M. Wickett (2005), Climate effects of global land cover change, *Geophys. Res. Lett.*, *32*, L23705, doi:10.1029/2005GL024550.

Hale, R. C., K. P. Gallo, T. W. Owen, and T. R. Loveland (2006), Land use/land cover change effects on temperature trends at U.S. Climate Normals stations, *Geophys. Res. Lett.*, *33*, L11703, doi:10.1029/2006GL026358.

Hansen, J., M. Sato, and R. Ruedy (1997), Radiative forcing and climate response, *J. Geophys. Res.*, *102*(D6), 6831–6864, doi:10.1029/96JD03436.

Intergovernmental Panel on Climate Change (IPCC) (2007), *Climate Change 2007: The Physical Science Basis, Contribution of Working Group I to the Fourth Assessment Report of the Intergovernmental Panel on Climate Change*, edited by S. Solomon et al., 996 pp., Cambridge Univ. Press, New York.

Jin, Y., and D. P. Roy (2005), Fire-induced albedo change and its radiative forcing at the surface in northern Australia, *Geophys. Res. Lett.*, *32*, L13401, doi:10.1029/2005GL022822.

Jin, Y., C. B. Schaaf, F. Gao, X. Li, A. H. Strahler, X. Zeng, and R. E. Dickinson (2002), How does snow impact the albedo of vegetated land surfaces as analyzed with MODIS data?, *Geophys. Res. Lett.*, *29*(10), 1374, doi:10.1029/2001GL014132.

Kleidon, A. (2006), The climate sensitivity to human appropriation of vegetation productivity and its thermodynamic characterization, *Global Planet. Change*, *54*, 109–127.

Loveland, T. R., T. L. Sohl, S. V. Stehman, A. L. Gallant, K. L. Sayler, and D. E. Napton (2002), A strategy for estimating the rates of recent United States land cover changes, *Photo. Eng. Remote Sens.*, *68*, 1091–1099.

Matthews, H. D., A. J. Weaver, M. Eby, and K. J. Meissner (2003), Radiative forcing of climate by historical land cover change, *Geophys. Res. Lett.*, *30*(2), 1055, doi:10.1029/2002GL016098.

Myhre, G., M. Kvalevag, and C. Schaaf (2005), Radiative forcing due to anthropogenic vegetation change based on MODIS surface albedo data, *Geophys. Res. Lett.*, *32*, L21410, doi:10.1029/2005GL024004.

National Research Council (2005), *Radiative Forcing of Climate Change: Expanding the Concept and Addressing Uncertainties*, 207 pp., Natl. Acad., Washington, D.C.

Oleson, K. W., G. B. Bonan, S. Levis, and M. Vertenstein (2004), Effects of land use change on North American climate: Impacts of surface datasets and model biogeophysics, *Clim. Dyn.*, *23*, 117–132.

Pielke, R. A., G. Marland, R. A. Betts, T. N. Chase, J. L. Eastman, J. O. Niles, D. D. S. Niyogi, and S. W. Running (2002), The influence of land-use change and landscape dynamics on the climate system: Relevance to climate-change policy beyond the radiative effect of greenhouse gases, *Philos. Trans. R. Soc. London, Ser. A*, *360*, 1705–1719.

Randerson, J. T., et al. (2006), The impact of boreal forest fire on climate warming, *Science*, *314*, 1130–1132.

Roy, D. P., P. Lewis, C. Schaaf, S. Devadiga, and L. Boschetti (2006), The Global impact of cloud on the production of MODIS bi-directional reflectance model based composites for terrestrial monitoring, *IEEE Geosci. Remote Sens. Lett.*, *3*, 452–456.

Schaaf, C. B., et al. (2002), First operational BRDF, albedo and nadir reflectance products from MODIS, *Remote Sens. Environ.*, *83*, 135–148.

Serra, J. (1982), *Image Analysis and Mathematical Morphology*, Academic, London.

Stehman, S. V., T. L. Sohl, and T. R. Loveland (2005), An evaluation of sampling strategies to improve precision of estimates of gross change in land use and land cover, *Int. J. Remote. Sens.*, *26*, 4941–4957.

Theobald, D. M. (2005), Landscape patterns of exurban growth in the USA from 1980 to 2020, *Ecol. Soc.*, *10*(1), 32.

C. A. Barnes and D. P. Roy, Geographical Information Science Center of Excellence, South Dakota State University, Brookings, SD 57007, USA. (christopher.barnes@sdstate.edu; david.roy@sdstate.edu)